Materials Chemistry and Physics 156 (2015) 214–219

Contents lists available at ScienceDirect

Materials Chemistry and Physics

journal homepage: www.elsevier.com/locate/matchemphys

Emission tunability and local environment in europium-doped OH^--free calcium aluminosilicate glasses for artificial lighting applications

Aline M. Farias [a], Marcelo Sandrini [a], José Renato M. Viana [a], Mauro L. Baesso [a], Antônio C. Bento [a], Jurandir H. Rohling [a], Yannick Guyot [b], Dominique De Ligny [c], Luiz Antônio O. Nunes [d], Flávio G. Gandra [e], Juraci A. Sampaio [f], Sandro M. Lima [g], Luis Humberto C. Andrade [g], Antônio N. Medina [a, *]

[a] Departamento de Física, Universidade Estadual de Maringá, Av Colombo, 5790, 87020-900, Maringá, PR, Brazil
[b] Laboratoire de Physico–Chimie des Matériaux Luminescents, Université de Lyon, Université Claude Bernard Lyon 1, Villeurbanne, UMR 5620 CNRS 69622, France
[c] Department of Materials Science and Engineering, University of Erlangen Nürnberg, Martens str. 5, 91058, Erlangen, Germany
[d] Instituto de Física de São Carlos, Universidade de São Paulo, Av. Trabalhador São-Carlense400, 13566-590, São Carlos, SP, Brazil
[e] Instituto de Física Gleb Wataghin, Universidade Estadual de Campinas, 13083-859, Campinas, SP, Brazil
[f] Lab Ciências Físicas, Universidade Estadual Norte Fluminense, 28013-602, Campos Dos Goytacazes, RJ, Brazil
[g] Grupo de Espectroscopia Óptica e Fototérmica, Universidade Estadual de Mato Grosso do Sul-UEMS, Dourados, MS, C. P. 351, CEP 79804-970, Brazil

HIGHLIGHTS

- Eu^{2+}-doped OH^- free calcium aluminosilicate glass as a new source for white lighting.
- Correlation between emission tunability and local environment of europium ions.
- Significant reduction of Eu^{3+} to Eu^{2+} by melting the glasses under vacuum atmosphere.
- Broad, intense and tunable luminescence ranging from blue to red.

ARTICLE INFO

Article history:
Received 24 July 2014
Received in revised form
23 February 2015
Accepted 1 March 2015
Available online 9 March 2015

Keywords:
Glasses
Luminescence
Optical properties
XAFS (EXAFS and XANES)
Photoluminescence spectroscopy
Visible and ultraviolet spectrometers

ABSTRACT

The relationship between emission tunability and the local environment of europium ions in OH^--free calcium aluminosilicate glasses was investigated, focusing on the development of devices for artificial lighting. Significant conversion of Eu^{3+} to Eu^{2+} was obtained by means of melting the glasses under a vacuum atmosphere and controlling the silica content, resulting in broad, intense, and tunable luminescence ranging from blue to red. Electron spin resonance and X-ray absorption near edge structure measurements enabled correlation of the luminescence behavior of the material with the Eu^{2+}/Eu^{3+} concentration ratio and changes in the surrounding ions' crystal field. The coordinates of the CIE 1931 chromaticity diagram were calculated from the spectra, and the contour maps showed that the light emitted from Eu^{2+} presented broad bands and enhanced color tuning, ranging from reddish-orange to blue. The results showed that these Eu doped glasses can be used for tunable white lighting by combining matrix composition and the adjustment of the pumping wavelength.

1. Introduction

A major challenge in the development of a new generation of artificial lighting is the tailoring of phosphor materials that possess efficient and tunable emissions across the whole range of the visible spectrum [1–7]. Europium and cerium are currently the most widely used phosphors in devices for lighting and displays, and both can coexist in several oxidation states in the host matrices. In addition, their emissions are known to be strongly dependent on the surrounding ions' crystal field [2].

* Corresponding author.
E-mail address: medina@dfi.uem.br (A.N. Medina).

http://dx.doi.org/10.1016/j.matchemphys.2015.03.002
0254-0584/

There are several factors that determine the luminescence properties of a material, such as the phonon energy, the presence of impurities, the nature and intensity of the surrounding crystal field, the oxidation states of the sensitizer ions, the synthesis procedure, and the morphology and geometry of the final material. From the point of view of materials science, tailoring of the surrounding ions' crystal field is essential in order to control the luminescence behavior. Consequently, many different materials have been developed for solid-state lighting, including crystals [2], ceramics [8], polymers [3,9], and glasses [1,7,10–12]. Specifically, the amorphous nature of glasses means that their broad luminescence properties are influenced by the average local crystal field surrounding the dopant ions. Selection of the matrix composition, the phosphor doping level, and the melting procedure are important ways of obtaining the desired emission characteristics.

We recently proposed the use of OH^--free low-silica calcium aluminosilicate (LSCAS) glass as an alternative luminescent material for tunable white lighting, due to its intense and broad emission spectrum in the visible region. These studies employed systems doped with Ce [7,12], Eu [10], and Ce–Eu [11]. The results revealed a significant influence of melting under a vacuum atmosphere on the production of glasses with ions in reduced oxidation states and with minimal presence of OH^- in their structures. This LSCAS glass is known to have superior thermo-mechanical properties, good chemical resistance, transparency from the UV–visible to the near infrared (up to 5 μm), reduced oxidation states for some dopant ions, and efficient laser emissions [13–18].

The certification of visible light sources for artificial lighting can employ parameters such as the correlated color temperature (CCT), the color rendering index (CRI), and the distance from the Planckian locus to the (u', v') color coordinates. The latter is known as Du'v' and describes how close the tested light source is in relation to the ideal lighting. These parameters, which characterize the emission, can be used to evaluate the melting procedure and the changes in composition, in order to optimize the glass luminescence. To this end, knowledge of the oxidation states of the sensitizer ions and the nature of the surrounding crystal field are important for tailoring the intended luminescent source.

Given the above considerations, this work therefore involved the development of a set of OH^--free Eu-doped aluminosilicate glasses with different silica contents. Investigation was made of the influence of the surrounding ions' crystal field and their oxidation states on the luminescence properties. The techniques used for characterization of the samples were electron spin resonance (ESR), X-ray absorption near edge structure (XANES), and photoluminescence (PL).

Table 1
Compositions (wt%), theoretical % of non-bridging oxygen (NBO), and optical basicity (Λ_{th}) of the glasses.

Samples	CaO	Al_2O_3	SiO_2	MgO	Eu_2O_3	NBO (%)	Λ_{th}
LSCAS	47.4	39.0	7.0	4.1	2.5	48.07	0.74
CAS 10	45.9	37.5	10.0	4.1	2.5	46.47	0.73
CAS 15	43.4	35.0	15.0	4.1	2.5	43.89	0.71
CAS 20	40.9	32.5	20.0	4.1	2.5	41.41	0.69
CAS 30	35.9	27.5	30.0	4.1	2.5	36.73	0.66
CAS 34	33.9	25.5	34.0	4.1	2.5	34.96	0.65
CAS 40	30.9	22.5	40.0	4.1	2.5	32.40	0.63
CAS 45	28.4	20.0	45.0	4.1	2.5	30.34	0.62
CAS 50	25.9	17.5	50.0	4.1	2.5	28.36	0.60
CAS 55	23.4	15.0	55.0	4.1	2.5	26.45	0.59
CAS 60	20.9	12.5	60.0	4.1	2.5	24.60	0.57
CAS 65	18.4	10.5	65.0	4.1	2.5	22.81	0.56

2. Experimental

High purity reagents (>99.995%) were used to prepare the glass samples. Table 1 shows the compositions (in wt%) required in order to obtain 6 g of the glasses. The reagents were mixed in a ball mill for 12 h, after which the mixtures were melted in graphite crucibles for 2 h under a vacuum atmosphere (10^{-3} mbar), at temperatures between 1400 °C and 1600 °C, according to the specific composition. Quenching was achieved by switching off the heater and moving the crucible up to a cooled vacuum chamber. Annealing was then performed by returning the crucible to the melting position, where the temperature was around 800 °C, and allowing it cool to room temperature, while maintaining the vacuum. This procedure took about 5 h. Further details of the preparation process can be found elsewhere [15,18]. The glass samples presented good optical quality, with no evidence of crystallization. They were cut and optically polished for the luminescence and XANES measurements, while for ESR the samples were in the form of powders.

ESR measurements were performed at room temperature using the microwave in the X-band spectral region ($\nu = 9.52$ GHz), with a power of 5 mW and a 10 Gauss amplitude modulated field at 100 kHz.

X-ray LIII edge (6977 eV) absorption spectra were measured using the D04B-XAFS2 beamline of the Brazilian National Synchrotron Light Laboratory (Laboratório Nacional de Luz Sincroton, LNLS) in Campinas, Brazil). The XANES spectra were collected in fluorescence mode using a Canberra GL0055S LEGe detector with an array of 15 elements [19]. The data were acquired as the averages of three scans for each sample. Excitation/emission contour maps were obtained using a Xe^+ lamp as the excitation source, with the wavelengths selected by a JobinYvon H10D monochromator. The excitation beam was focused on the sample and the emission was collected by means of an optical fiber and detected by a CCD array connected to a microcomputer. Luminescence measurements were also carried out using an Ar^+ ion laser at 355 nm - 365 nm and a diode laser at 532 nm as excitation sources, with detection by a silicon photodiode. The detection system was calibrated by using an irradiance and illuminance standard source (from the National Institute of Standards and Technology, NIST) from Gooch & Housego, model 752-10 E.

3. Results and discussion

Fig. 1 shows the ESR spectra as a function of the silica content. The data were normalized in terms of the Eu_2O_3 weight. Eu^{3+} ions

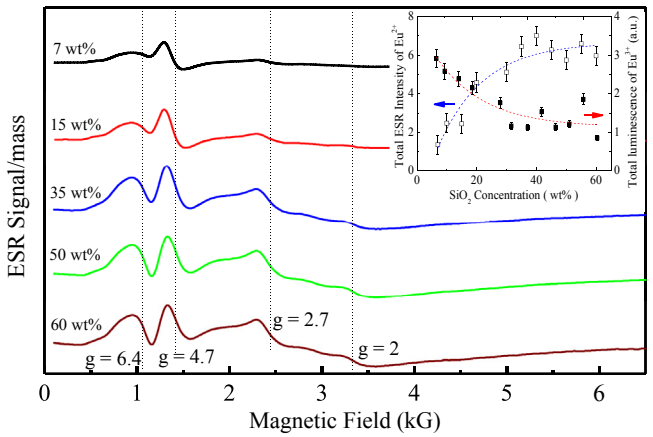

Fig. 1. Normalized ESR spectra for the samples with 7, 15, 34, 50, and 60 wt% of silica. The inset shows the integrated areas of the ESR absorption spectra and the selective Eu^{3+} total luminescence obtained by pumping the samples at 532 nm.

are not paramagnetic, so could not be detected in the ESR measurements. On the other hand, Eu^{2+} has electronic spin S 7/2, enabling evaluation of the $^8S_{7/2}$ singlet ground state by this technique. Using 2,2-diphenyl-1-picrylhydrazyl (dpph) as a reference pattern, the ESR signal intensity was considered to be proportional to the amount of Eu^{2+} ions in the sample. It can be seen (Fig. 1) that there were resonance lines with g 2, 2.7, 4.7, and 6.4, and that the signal intensity increased for higher silica contents (inset of Fig. 1). This reflected an increase in the Eu^{2+}/Eu^{3+} ratio, because the total amount of europium in the sample remained constant.

The resonance lines at g 6, 2.7, and 2 are known as the characteristic U spectrum for Gd^{3+} and Eu^{2+} used as dopants in glasses or disordered polycrystalline materials [20,21]. The existence of several resonance lines, as opposed to just one at g 2.0, as observed in the ESR spectra of rare earth ions in the S state, has been used to demonstrate that Gd^{3+}, Eu^{2+}, and Tb^{4+} present different interactions with the crystal matrix fields [20,22]. Iton and Brodbeck [21] simulated the ESR spectra of Gd^{3+} and Eu^{2+} in zeolites and compared the results with experimental data obtained in the X band. They proposed that the U spectrum lines indicated the occurrence of a moderate distortion of the crystal field in relation to the cubic, tetrahedral, or octahedral basic structures. It was observed that the detected distortions were predominant when the ions were in a high coordination number (>6). On the other hand, resonance at g 4.86 is indicative of a crystal field with orthorhombic symmetry and strong interaction between the ions, as shown by Iton and Turkevich [23]. Additionally, ESR spectra of both Gd^{3+} and Eu^{2+} in glasses, measured at low microwave frequency, have shown reduced intensities of the $g \approx 6$ U spectra, together with the generation of a broad line at around $g \approx 5$ [24,25]. From Fig. 1, it can be seen that with the increase of silica content, the intensities of lines related to the U spectrum increased considerably, relative to that for resonance at g 4.7. This suggests that in addition to promoting the reduction $Eu^{3+} \rightarrow Eu^{2+}$, the addition of silica resulted in the formation of weaker crystal field interactions in the sites surrounding the Eu^{2+} ions.

Fig. 2 shows the normalized X-ray absorption spectra as a function of the energy in the XANES region. Two absorption peaks were observed, with differences in energy of about 8 eV, reflecting a hybrid structure with the existence of two europium valence states in the glasses [26]. The peak at lower energy was characteristic of Eu^{2+}, while that at higher energy was characteristic of the Eu^{3+} ions

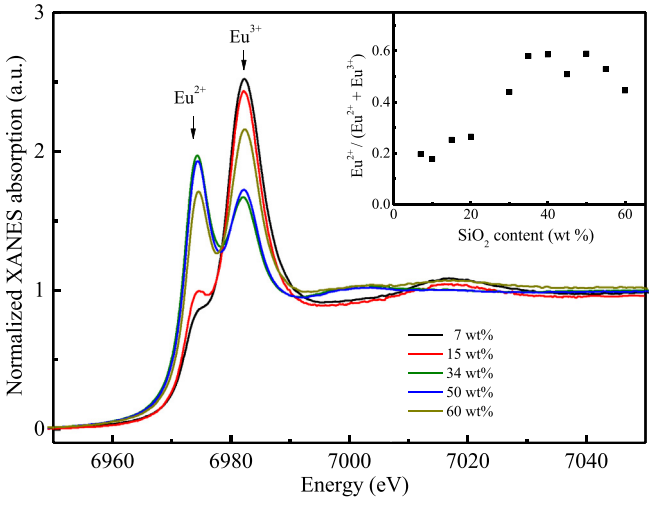

Fig. 2. LIII edge XANES spectrum (6977 eV) of europium ions in the samples with 7, 15, 34, 50, and 60 wt% of silica. The inset shows the Eu^{2+} fraction for different silica contents.

[27]. A higher silica content in the matrices resulted in increased intensity of the Eu^{2+} peak and consequently a reduction in the contribution from the Eu^{3+} ions. The averaging was done by performing three scans in each sample and the spectra were fitting using the Athena software (IFFEFIT package) [28]. As europium shows separate absorption edges related to the Eu^{2+} and Eu^{3+} ions, two arctangent functions were used to fit the step energy observed in the spectra, and two Gaussian functions were used to fit the peaks. The inset of Fig. 2 shows the amount of Eu^{2+} as a function of the silica content, from which it can be seen that the amount increased up to three-fold at higher silica concentrations. This behavior was in agreement with the ESR data. The coexistence of Eu^{2+} and Eu^{3+} in OH^--free LSCAS glass has been reported previously [10,11,29]. In an earlier study [29], overlapping of the emission lines between 570 and 750 nm was observed, attributed to the $^5D_0 \rightarrow {}^7F_J$ (J 0, 1, 2, 3, and 4) transitions of the Eu^{3+} ion. The observed broad emission band centered at 585 nm was attributed to the $^4F_6 \rightarrow {}^4F_7$ transition of the Eu^{2+} ion.

Fig. 3 shows the luminescence spectra for excitation at 350 nm. For the samples with lower silica concentrations, there were narrow emission peaks due to Eu^{3+} and a broad peak in the red-orange region due to Eu^{2+}. For higher silica concentrations, there were increases of about 400-fold in the intensity of the emission band related to Eu^{2+}, and the emission peak shifted to the blue region. This significant increase was related to the greater quantities of divalent ions in the samples with higher silica contents, as indicated by the inset in Fig. 2. The Eu^{2+}/Eu^{3+} ratio is expected to decrease considerably at low silica contents, so it becomes easy to observe the Eu^{3+} emission in Fig. 3. For all the samples, the selective Eu^{3+} luminescence was measured using excitation at 532 nm. The results did not show any changes in the relative intensities of the bands, according to the silica content. However, as expected, a decrease in the total intensity was observed (shown in the inset of Fig. 1). The observed behavior was like a mirror, compared to the ESR intensity. Although the use of 350 nm does not directly excite Eu^{3+}, energy transfer from Eu^{2+} to Eu^{3+} by reabsorption is possible, due to the overlap among Eu^{2+} absorption bands and Eu^{3+} absorption lines, as reported recently [10].

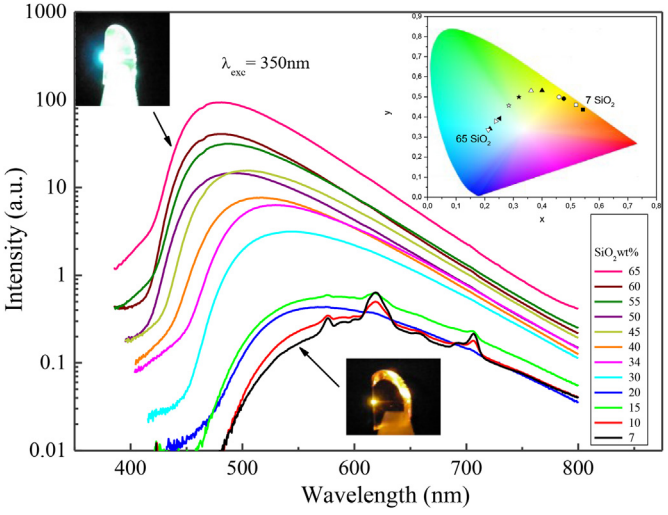

Fig. 3. Luminescence spectra for the samples with different silica concentrations. The excitation was at 350 nm. The photographs show the different luminescence colors obtained for the samples with the lowest and highest silica concentrations. The inset shows the chromaticity diagram, with identification of the color of light emitted from each sample, without considering any complementary blue emission from the pumping source. (For interpretation of the references to color in this figure legend, the reader is referred to the web version of this article.)

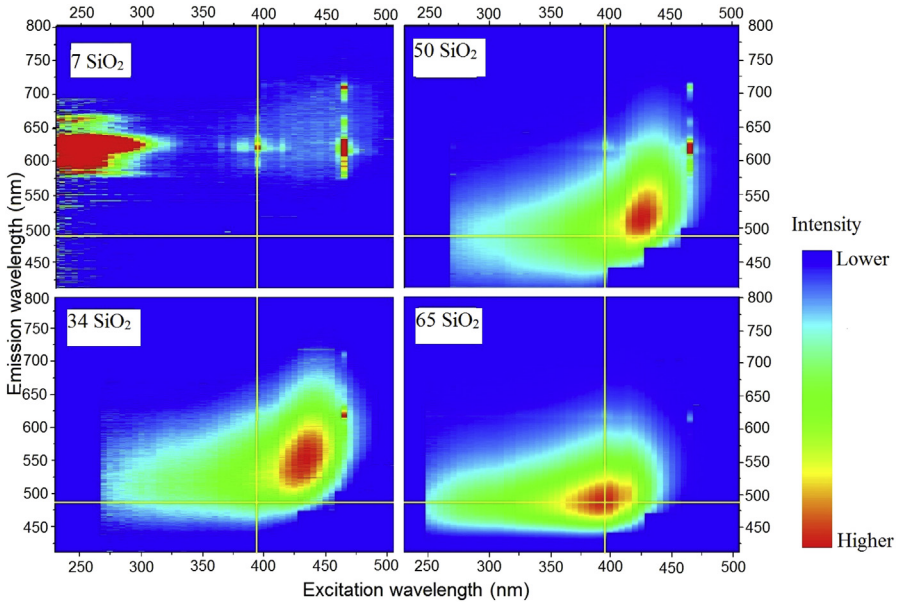

Fig. 4. Contour plots of excitation/emission spectra for the samples with 7, 34, 50, and 65 wt% of silica.

Wang et al. [30] suggested that a decrease in the Eu^{2+} emission intensity can result from an increase in the number of non-bridging oxygens (NBOs), caused by a greater number of negative charges in the glass network. This favors the formation of ions with higher valence states, maintaining the neutrality of the material. It has been shown previously that the quantity of NBOs in calcium aluminosilicate glasses decreases when the amount of silica in the matrix is increased [31]. A calculation assuming all Ca and Mg to be modifiers and all Al and Si to be network formers was used to estimate the theoretical %NBO. The results (Table 1) showed that from the lowest to highest silica contents, the %NBO changed from 48% to 23%. Therefore, the increase in the Eu^{2+} emission intensity at higher silica contents was in agreement with the data published previously.

The red shift of the emission band of Eu^{2+} is often associated with the optical basicity of the glass (Λ_{th}). Following the work of Duffy and Infram [32], a theoretical optical basicity can be calculated for the glass studied here (Table 1). The increase in the optical basicity from 0.56 to 0.74, with decrease of the silica content, suggests that the crystal field strength of the glass was higher, resulting in a splitting of the Eu^{2+} d orbital degeneracy [33,34]. This would result in separation of the two energy levels, with e_g and t_{2g} shifting to lower and higher energy, respectively [33,34]. In other words, the separation between these two bands depends on the strength of this interaction. In addition, a large separation implies a connection between the lower level (e_g) and the ground state 4f, resulting in emission with lower energy, at longer wavelengths. A similar red shift was also observed for Ce^{3+}-doped LSCAS [7,12]. According to Novatski et al. [31], and in agreement with the estimated values given in Table 1, the optical basicity decreases when the silica concentration increases, so there is a decrease in the separation of the e_g and t_{2g} bands, and consequently an increase in the separation between the ground state and the e_g band. Thus, by increasing the concentration of silica, the emission peaks shift to lower wavelengths, as shown in Fig. 3. The decrease of the crystal field interaction with the d orbitals, as suggested by the emission results, is in agreement with the increasing intensity of the U spectrum observed in the ESR data.

The coordinates in the CIE 1931 chromaticity diagram were calculated from the emission spectra, as shown in the inset of Fig. 3. It can be observed that at higher silica contents, there was a shift in the emitted color from the orange-red region to the blue region.

Table 2
CRI, CQS, CCT, and Du'v' parameters as a function of silica content, in wt%.

Samples	CRI		CQS		CCT		Du'v'	
	λ_{ex1}	λ_{ex2}	λ_{ex1}	λ_{ex2}	λ_{ex1}	λ_{ex2}	λ_{ex1}	λ_{ex2}
LSCAS	72	76	2	49	1930	1487	0.008	−0.001
CAS 10	64	77	2	18	2290	1634	0.014	0.004
CAS 15	57	79	7	31	2900	2012	0.033	0.008
CAS 20	54	77	8	34	3100	2424	0.040	0.014
CAS 30	48	67	28	37	3900	3346	0.062	0.031
CAS 34	47	68	36	49	3900	3784	0.062	0.036
CAS 40	50	64	46	51	5050	4340	0.077	0.045
CAS 45	50	68	53	63	5950	5131	0.076	0.047
CAS 50	57	65	58	62	7600	5515	0.067	0.052
CAS 55	55	65	57	65	8400	6297	0.069	0.051
CAS 60	–	68	–	67	>10000	7193	0.066	0.048
CAS 65	–	66	–	66	>10000	7459	0.068	0.051

λ_{ex1} 350 nm; λ_{ex2} 399 nm.

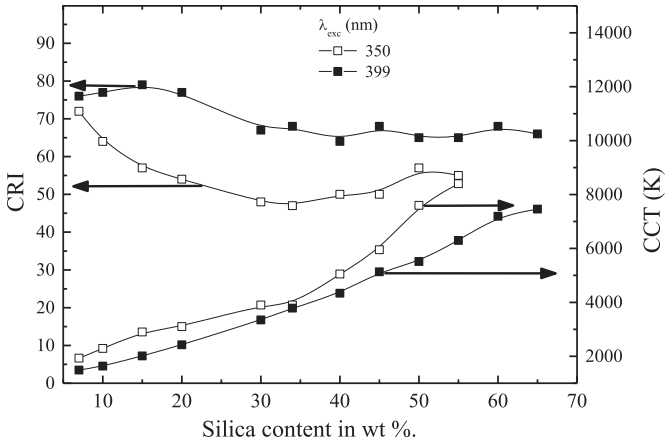

Fig. 5. Correlated color temperature (CCT) and color rendering index (CRI), as a function of silica content.

This blue shift in the maximum emission intensity contributes to reduce the CRI values and to increase the CCT values for glasses with high silica. The photographs in Fig. 3 illustrate the differences between the emissions.

Fig. 4 shows contour plots of the excitation/emission spectra for the samples with 7, 35, 50, and 65 wt% of silica. As described above, the luminescence intensity is very different among the samples, so that in the figure they cannot be compared in intensity. In fact, only the maximum positions for the excitation and emission wavelengths can be checked. For the sample with 7 wt% of silica, the Eu^{2+} emission was much lower than that of Eu^{3+}, while the Eu^{2+} emissions became more evident at higher silica concentrations. The plots indicated that the blue shift of the emission band observed for excitation at 350 nm also occurred for other excitation wavelengths. The excitation band showed similar behavior. The information obtained from the excitation/emission contour plots indicated that it was possible to tune the emission by modifying the oxidation states of the ions and/or the crystal matrix field.

The calculated values of the CRI, CQS, CCT, and Du'v' parameters are shown in Table 2 and Fig. 5. The color changes were reflected by both an increase in Du'v' and a decrease in the CCT values. The Du'v' values lay outside the acceptable maximum of 0.006 established by the American National Standards Institute (ANSI C-78.377). However, for silica contents lower than 20%, the values complied with the Du'v' limit value of <0.02 set by the Japanese Standards Association (JIS C-8152-2). It is important to note that these comparisons were made without considering complementary emissions from blue LEDs, which could be used for the construction of WLED devices. This would make it possible to obtain parameter values within the ranges established in current technical standards. It can be seen that there were substantial differences between the CRI and color quality scale (CQS) values (Table 2). The CQS is a new color quality parameter that is now accepted by NIST. It is considered superior for the measurement of color quality because it employs 15 standard pastel colors as a reference for color reproducibility, while the CRI uses only 8 standard colors. It is known that for some deep red color spectra, the CRI can give inaccurate results. This can be seen by comparing the CQS and CRI values (Table 2) for the aluminosilicate samples with low silica contents, which presented a red color under UV and violet excitation and showed the greatest differences between the CRI and CQS values. Despite this divergence between the CRI and CQS techniques, the CRI remains the internationally accepted parameter, according to the Commission on Illumination (CIE), and for much of the visible band there were only small differences between the CRI and CQS values.

4. Conclusions

In conclusion, the results showed the coexistence of Eu^{2+} and Eu^{3+} oxidation states in the aluminosilicate glasses analyzed here. It was observed that with increasing silica concentration, the matrix promoted the conversion $Eu^{3+} \rightarrow Eu^{2+}$, which was associated with changes in the optical basicity of the matrix and the amount of NBO. The ESR and luminescence results indicated that the addition of silica induced changes in the europium valence states, as well as modifications in the Eu^{2+} sites symmetry. For excitation at 350 nm, a broad emission band from the Eu^{2+} ions was observed, with a peak shift from 585 to 480 nm, resulting in the color of the emitted light changing from reddish-orange to blue. This shift to higher energies occurred for both emission and excitation bands. The present observations indicate that these Eu-doped glasses can be tailored for tunable white lighting by combining adjustment of the matrix composition, melting environment, and pumping wavelength.

Acknowledgments

The authors are grateful to the Brazil/France CAPES/COFECUB program (grant no. 565/2007), CNPq (grant no. 484969/2013-7), Fundação Araucária (grant no. 23309/2012), FINEP (grant no. 0861/10), LNLS (XAS1/11839), and UCBLyon1-CNRS for financial support.

References

[1] J. He, Y. Wang, Y. Liu, K. Wang, R. Li, J. Fan, S. Xu, L. Zhang, Tailoring the luminescence of europium ions in mesoporous $AlPO_4$ monolithic glass, J. Phys. Chem. C 117 (2013) 21916–21922.
[2] Z. Xia, Y. Zhang, M.S. Molokeev, V.V. Atuchin, Structural and luminescence properties of yellow-emitting $NaScSi_2O_6$: Eu^{2+} phosphors: Eu^{2+} site preference analysis and generation of red emission by codoping Mn^{2+} for white-light-emitting diode applications, J. Phys. Chem. C 117 (2013) 20847–20854.
[3] H.S. Jang, H. Yang, S.W. Kim, J.Y. Han, S.-G. Lee, D.Y. Jeon, White light-emitting diodes with excellent color rendering based on organically capped CdSe quantum dots and Sr_3SiO_5:Ce^{3+}, Li^+ phosphors, Adv. Mat. 20 (2008) 2696–2702.
[4] H.S. Jang, W. Bin Im, D.C. Lee, D.Y. Jeon, S.S. Kim, Enhancement of red spectral emission intensity of $Y_3Al_5O_{12}$: Ce^{3+} phosphor via Pr co-doping and Tb substitution for the application to white LEDs, J. Lumin. 126 (2007) 371–377.
[5] E.F. Schubert, J.K. Kim, Solid-state light sources getting smart, Science 308 (2005) 1274–1278.
[6] X. Xu, X. Yu, D. Zhou, J. Qiu, A potential tunable blue-to-white-emitting phosphor CAO: Eu, Mn for ultraviolet light emitting diodes, Mat. Res. Bull. 48 (2013) 2390–2392.
[7] L.H.C. Andrade, S.M. Lima, A. Novatski, A. Steimacher, J.H. Rohling, A.N. Medina, A.C. Bento, M.L. Baesso, Y. Guyot, G. Boulon, A step forward toward smart white lighting: combination of glass phosphor and light emitting diodes, Appl. Phys. Lett. 95 (2009) 081104.
[8] L.G.D. Silveira, L.F. Cotica, I.A. Santos, M.P. Belancon, J.H. Rohling, M.L. Baesso, Processing and luminescence properties of Ce:$Y_3Al_5O_{12}$ and Eu:$Y_3Al_5O_{12}$ ceramics for white-light applications, Mat. Lett. 89 (2012) 86–89.
[9] C. Fan, L. Zhu, B. Jiang, Y. Li, F. Zhao, D. Ma, J. Qin, C. Yang, High power efficiency yellow phosphorescent OLEDs by using new iridium complexes with halogen-substituted 2-phenylbenzo[d]thiazole ligands, J. Phys. Chem. C 117 (2013) 19134–19141.
[10] S.M. Lima, L.H.C. Andrade, J.R. Silva, A.C. Bento, M.L. Baesso, J.A. Sampaio, L.A.O. Nunes, Y. Guyot, G. Boulon, Broad combined orange-red emissions from Eu^{2+} and Eu^{3+} doped low-silica calcium aluminosilicate glass, Opt. Exp. 20 (2012) 12658–12665.
[11] A.C.P. Rocha, L.H.C. Andrade, S.M. Lima, A.M. Farias, A.C. Bento, M.L. Baesso, Y. Guyot, G. Boulon, Tunable color temperature of Ce^{3+}/Eu^{2+}, Eu^{3+} co-doped low silica aluminosilicate glasses for white lighting, Opt. Exp. 20 (2012) 10034–10041.
[12] L.H.C. Andrade, S.M. Lima, M.L. Baesso, A. Novatski, J.H. Rohling, Y. Guyot, G. Boulon, Tunable light emission and similarities with garnet structure of Ce-doped LSCAS glass for white-light devices, J. Alloy Compd. 510 (2012) 54–59.
[13] L.H.C. Andrade, S.M. Lima, A. Novatski, P.T. Udo, N.G.C. Astrath, A.N. Medina, A.C. Bento, M.L. Baesso, Y. Guyot, G. Boulon, Long fluorescence lifetime of Ti^{3+}-doped low silica calcium aluminosilicate glass, Phys. Rev. Lett. 100 (2008) 027402.
[14] D.F. De Sousa, L.A.O. Nunes, J.H. Rohling, M.L. Baesso, Laser emission at 1077 nm in Nd^{3+}-doped calcium aluminosilicate glass, Appl. Phys. B Lasers Opt. 77 (2003) 59–63.
[15] Y. Guyot, A. Steimacher, M.P. Belancon, A.N. Medina, M.L. Baesso, S.M. Lima, L.H.C. Andrade, A. Brenier, A.M. Jurdyc, G. Boulon, Spectroscopic properties, concentration quenching, and laser investigations of Yb^{3+}-doped calcium aluminosilicate glasses, J. Opt. Soc. Am. B Opt. Phys. 28 (2011) 2510–2517.
[16] L.J. Borrero-Gonzáles, I.A.A. Terra, L.A.O. Nunes, A.M. Farias, M.J. Barboza, J.H. Rohling, A.N. Medina, M.L. Baesso, The influence of SiO_2 content on spectroscopic properties and laser emission efficiency of Yb^{3+}-Er^{3+} co-doped calcium aluminosilicate glasses, Appl. Phys. B 107 (2012) 415–420.
[17] D.F. de Souza, J.A. Sampaio, L.A.O. Nunes, M.L. Baesso, A.C. Bento, L.C.M. Miranda, Energy transfer and the 2.8-μm emission of Er^{3+} and Yb^{3+}-doped low silica content calcium aluminate glasses, Phys. Rev. B 62 (2000) 3176–3180.
[18] A. Steimacher, M.J. Barboza, A.M. Farias, O.A. Sakai, J.H. Rohling, A.C. Bento, M.L. Baesso, A.N. Medina, C.M. Lepienski, Preparation of Nd_2O_3-doped calcium aluminosilicate glasses and thermo-optical and mechanical characterization, J. Non-Cryst. Solids 354 (2008) 4749–4754.
[19] D.C. Koningsberger, X-ray Absorption: Principles, Applications, Techniques of EXAFS, SEXAFS and XANES, John Wiley & Sons, 1998.
[20] C.M. Brodbeck, L.E. Iton, The electron-paramagnetic-res spectra of Gd^{3+} and Eu^{2+} in glassy systems, J. Chem. Phys. 83 (1985) 4285–4299.
[21] L.E. Iton, C.M. Brodbeck, S.L. Suib, G.D. Stucky, EPR study of europium ions in type-A zeolite. The general classification of the EPR spectra of S-state rare-earth ions in disordered polycrystalline or glassy matrices, J. Chem. Phys. 79 (1983) 1185–1196.
[22] H. Ebendorff-Heidepriem, D. Ehrt, Electron spin resonance spectra of Eu^{2+} and

Tb^{4+} ions in glasses, J. Phys. Condens. Matter 11 (1999) 7627–7634.
[23] L.E. Iton, J. Turkevich, Electron paramagnetic resonance of rare-earth ions in zeolites, J. Phys. Chem. 81 (1977) 435–449.
[24] L. Cugunov, A. Mednis, J. Kliava, Multiband electron spin resonance spectroscopy of rare earth S-ions in glasses: the isospectral frequency ratio method, J. Phys. Condens. Matter. 3 (1991) 8017–8025.
[25] C. Legein, J.Y. Buzare, G. Silly, C. Jacoboni, The local field distribution of Gd^{3+} in transition metal fluoride glasses investigated by electron paramagnetic resonance, J. Phys. Condens. Matter 8 (1996) 4339–4350.
[26] G. Krill, X-ray absorption spectroscopy (L3 edges, XANES, EXAFS) on 4f mixed-valent compounds, J. de Physique: Colloque 47 (1986) 907–914.
[27] D. Malterre, A. Siari, J. Durand, G. Krill, G. Marchal, X-ray absorption spectroscopy on amorphous mixed-valent alloys, J. de Physique: Colloque 47 (1986) 991–995.
[28] B. Ravel, M. Newville, ATHENA, ARTEMIS, HEPHAESTUS: data analysis for x-ray absorption spectroscopy using IFEFFIT, J. Synchrotron Radiat. 12 (2005) 537–541.
[29] J.A. Sampaio, M.C. Filadelpho, A.A. Andrade, J.H. Rohling, A.N. Medina, A.C. Bento, L.M. da Silva, F.C.G. Gandra, L.A.O. Nunes, M.L. Baesso, Study on the observation of Eu^{2+} and Eu^{3+} valence states in low silica calcium aluminosilicate glasses, J. Phys. Condens. Matter 22 (2010) 055601.
[30] C. Wang, M.Y. Peng, N. Jiang, X.W. Jiang, C.J. Zhao, J.R. Qiu, Tunning the europium luminescence in glass materials synthesized in air by adjusting glass compositions, Mat. Lett. 61 (2007) 3608–3611.
[31] A. Novatski, A. Steimacher, A.N. Medina, A.C. Bento, M.L. Baesso, L.H.C. Andrade, S.M. Lima, Y. Guyot, G. Boulon, Relations among nonbridging oxygen, optical properties, optical basicity, and color center formation in CaO–MgO aluminosilicate glasses, J. Appl. Phys. 104 (2008) 094910.
[32] J.A. Duffy, M.D. Infram, An interpretation of glass chemistry in terms of the optical basicity concept, J. Non-Cryst. Solids 21 (1976) 373–410.
[33] S.M. Liu, G.L. Zhao, W.G. Ruan, Z.W. Yao, T.T. Xie, J. Jin, H. Ying, J.X. Wang, G.R. Han, Reduction of Eu^{3+} to Eu^{2+} in aluminoborosilicate glasses prepared in air, J. Am. Cer. Soc. 91 (2008) 2740–2742.
[34] M. Nogami, T. Yamazaki, Y. Abe, Fluorescence properties of Eu^{3+} and Eu^{2+} in Al_2O_3-SiO_2 glass, J. Lumin. 78 (1998) 63–68.